Ultrahigh-pressure scales for gold and platinum at pressures up to 550 GPa

Manabu Yokoo, Nobuaki Kawai, Kazutaka G. Nakamura, and Ken-ichi Kondo

Materials and Structures Laboratory, Tokyo Institute of Technology, 4259 Nagatsuta, Midori, Yokohama 226-8503, Japan

Yoshinori Tange and Taku Tsuchiya[*]

Geodynamics Research Center, Ehime University, 2-5 Bunkyo, Matsuyama 790-8577, Japan

Equation of state of gold (Au) is revised using the remeasured shock compression data at pressures up to 580 GPa with including the electronic free-energy contribution. The model, even though determined only using pressure-scale-free data, can reproduce not only the shock compression data but also the zero-pressure thermodynamic properties with remarkable accuracy. Previous models for the EOS of copper, silver, and MgO that were constructed using as a basis old shock compression data are found to underestimate the pressure seriously (up to ~12% at 200 GPa and 300 K). Moreover, we redetermine the EOS model of platinum (Pt) through the same procedure. The determined models of Au and Pt are found mutually highly consistent, which provide quite comparable pressure values in extensive *P*, *T* range. These are expected to be more reliable primary pressure standards than previous models.

PACS number(s): 62.50.Ef, 64.30.Ef

I. INTRODUCTION

In general, pressure is calibrated using pressure-dependent properties, such as lattice constants (or volume), luminescence spectra, and phase transition conditions of standard materials.[1–3] Empirical EOS for metals are quite practical for pressure measurements particularly above 100 GPa and shock compression data have been used to construct the *P*-*V*-*T* EOS as primary standards. Since shock-compressed states can be described within the fundamental conservation laws of mass, momentum, and energy, we can directly evaluate the pressure values independently from any scales. So far, the EOS of platinum (Pt) has been used as the highest-pressure scale up to ~500 GPa, which was determined based on the shock compression data to 660 GPa.[4]

Gold (Au) is recognized as one of the most useful standard materials because of its chemical inertness, efficient x-ray scattering property, high stability under extreme conditions, and high compressibility. However, several different EOS models have been proposed for Au and the discrepancy between them has often been argued as a central problem particularly in the Earth sciences.[5,6] Simultaneous static compression measurements revealed inconsistency in the pressure values determined from the Au and Pt EOS, which reaches at most 20 GPa up to 145 GPa.[7] Latest shock compression data for Au up to 580 GPa reported by a symmetric-impact experimental study using a two-stage light-gas gun suggested crucial underestimations in the previously obtained shock pressures.[8]

In this study, we first revised the *P*-*V*-*T* EOS of Au using our recent shock compression data up to 580 GPa[8] combining its atmospheric pressure-scale-independent thermal and elastic properties. Then, we also reanalyzed the shock compression data of Pt up to 660 GPa,[4] and evaluated their mutual consistency.

II. PRESSURE-VOLUME-TEMPERATURE EQUATION OF STATE OF GOLD

A. Model of equation of state

Parameters for the *P*-*V*-*T* EOS are determined using the Mie-Grüneisen formulation. In the Mie-Grüneisen approach for nonmagnetic metals such as Au and Pt, *P* at a given *V* and *T* can be approximated as a sum of zero-temperature pressure and thermal pressures given by the contributions of phonon thermal vibration and electronic thermal excitation:

$$P(V,T) = P_c(V,0) + P_{ph}(V,T) + P_{el}(V,T), \quad (1)$$

where the subscript *c* denotes the value at 0 K, and *ph* and *el* are the values associated with phonon and electron contributions, respectively. The internal energy $E(V,T)$ is also represented similarly.

P_c is given by the third-order Birch-Murnaghan equation,

$$P_c(V) = \frac{3}{2}B_0\left[\left(\frac{V}{V_c}\right)^{-7/3} - \left(\frac{V}{V_c}\right)^{-5/3}\right] \times \left\{1 + \frac{3}{4}(B_0'-4)\left[\left(\frac{V}{V_c}\right)^{-2/3} - 1\right]\right\}, \quad (2)$$

where B_0 and B_0' are the bulk modulus and its pressure derivative at 1 atm and 0 K, respectively. In the case of zero-temperature compression, the energy E_c can be represented as the volume integration of P_c,

$$E_c(V) = -\int P_c(V)dV. \quad (3)$$

P_{ph} and E_{ph} are evaluated using the Debye model. In this model, $E_{ph}(V,T)$ can be represented as

$$E_{ph}(V,T) = 3nk_BTD_3(x) \quad (4)$$

and

$$D_3(x) = \frac{3}{x^3}\int_0^x \frac{z^3}{e^z - 1}dz, \quad (5)$$

where $3nk_B$ is the Dulong-Petit value, $x = \Theta_D(V)/T$, Θ_D is the Debye temperature, and $D_3(x)$ is the Debye function. Once the Grüneisen parameter for the phonon contribution, γ_{ph}, is defined, Θ_D is known to be given by

$$\frac{d \ln \Theta_D}{d \ln V} = -\gamma_{ph}, \qquad (6)$$

where we assume γ_{ph} to be a function only of volume. The lattice specific heat $C_{v,ph}$ is given by

$$C_{v,ph}/3nk_B = 4D_3(x) - 3x/(e^x - 1). \qquad (7)$$

Therefore, in the Mie-Grüneisen formulation with the Debye model, the thermal pressure from the phonon contribution is

$$P_{ph}(V,T) = \frac{\gamma_{ph}(V)}{V} E_{ph}. \qquad (8)$$

The Grüneisen parameter γ_{ph} is often expressed assuming that q ($=d \ln \gamma_{ph}/d \ln V$) is constant, because the volume dependence of γ is still unclear. In this model, we obtain

$$\gamma_{ph}(V) = \gamma_0 \left(\frac{V}{V_0}\right)^q. \qquad (9)$$

Recently, it was clarified that this equation is too simple to be applied in broad P, V region.[9] In this study, we rather used a modified formulation proposed by Tange *et al.*,[9]

$$\gamma_{ph}(V) = \gamma_0\{1 + a[(V/V_0)^b - 1]\}, \qquad (10)$$

where γ_0 is the Grüneisen parameter under ambient conditions and the constants a and b are volume-independent parameters. This is more flexibly applicable to represent the volume dependence of γ_{ph} compared to Eq. (9). When $a=1$, Eq. (10) is equivalent to the conventional expression of Eq. (9). In Eq. (10), γ_{ph} approaches a constant value, $(1-a)\gamma_0$, at infinite compression ($V \to 0$), and thus a should be in $0 \leq a \leq 1$. Corresponding to q in Eq. (9), q_{ph} can be defined in this case as

$$q_{ph}(V) = \frac{ab(V/V_0)^b}{1 + a[(V/V_0)^b - 1]}. \qquad (11)$$

When $V=V_0$, q_{ph} becomes equal to the product of the constants a and b. The Debye temperature can simply be calculated by the integration of Eq. (6),

$$\Theta_D(V) = \Theta_0 \left(\frac{V}{V_0}\right)^{-(1-a)\gamma_0} \exp\left[-\frac{\gamma_{ph}(V) - \gamma_0}{b}\right]. \qquad (12)$$

The electronic effect is not negligible in the shock-compressed states of metal, which reach more than $\sim 10^2$ GPa and $\sim 10^4$ K, and the electronic thermal pressure P_{el} and energy E_{el} were predicted by first-principles electronic structure calculations for Au and Pt.[10] Once E_{el} is determined at a given V and T, the electronic specific heat $C_{v,el}$ can be calculated from $(\partial E_{el}/\partial T)_V$. Thus, the total specific heat of nonmagnetic metals is obtained by the sum of $C_{v,ph}$ and $C_{v,el}$.

B. Shock compression

Figure 1 shows the experimental shock compression velocity U_s and particle velocity u_p of Au along the Hugoniot.[8,11–13] Among them, data measured by the 1960s were based on different standards at each laboratory, whose
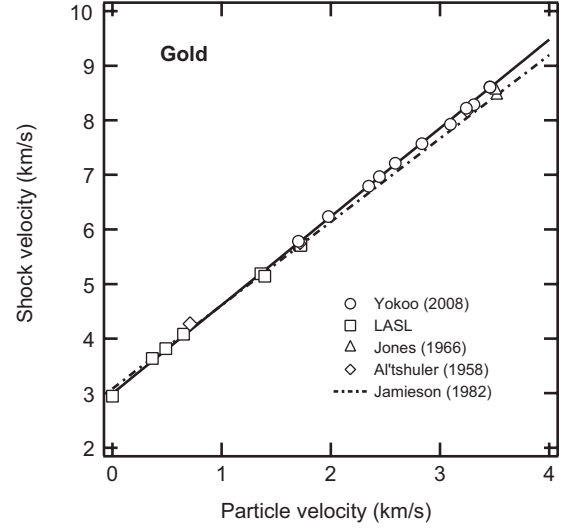
FIG. 1. Relationship between the shock velocity (U_s) and particle velocity (u_p) of Au. Solid and dashed curves indicate the relationships obtained in this work using shock compression data (Ref. 8) and reported in Jamieson *et al.* (Ref. 3), respectively.

uncertainties are currently unclear.[3] Shock compression data were however recently obtained by a symmetric-impact experiment using a two-stage light-gas gun and a line-reflection method up to 580 GPa with uncertainty of U_s at most $\sim 2\%$.[8] This study demonstrated that U_s was underestimated in the early shock compression experiments.[3,11–13]

In principle, U_s is identical to the bulk sound velocity C_0 at $u_p = 0$ km/s when a sample is in the hydrostatic state without stress relaxation or strain hardening. Elastic constants reported by single-crystal ultrasonic measurements[14,15] supply $C_0 = 2.995$ km/s. Using these data, we reoptimized the $U_s - u_p$ relationship of Au in the range of $u_p \leq 3.5$ km/s in quadratic form as

$$U_s = 2.995 + 1.653u_p - 0.013u_p^2, \qquad (13)$$

where the uncertainties of coefficients are ± 0.056 and ± 0.019 (km/s)$^{-1}$ within 2σ, respectively. The data deviate around 0.40% on average, and 2σ of U_s is found less than $\pm 1.0\%$. Figure 1 also shows the previous U_s-u_p relationships,[3] $U_s = 2.975 + 1.896u_p - 0.309u_p^2$ ($u_p \leq 0.4132$ km/s) and $U_s = 3.071 + 1.536u_p$ ($u_p \geq 0.4132$ km/s), which give a markedly slower U_s at most 2.3% for $0 \leq u_p \leq 3.5$ km/s. This difference is greater than the fitting error.

The Rankine-Hugoniot equations based on the conservation laws of mass, momentum and energy are used for the analyses of P-V-E relationships in the shock-compressed states. In the case of materials initially at rest, they are

$$V_h/V_0 = 1 - u_p/U_s, \qquad (14)$$

$$P_h - P_0 = \rho_0 U_s u_p, \qquad (15)$$

$$E_h - E_0 = (P_h + P_0)(V_0 - V_h)/2, \qquad (16)$$

TABLE I. Volume and temperature ranges of the experimental thermodynamic properties at 1 atm used for the determination of EOS parameters of Au. Values in parentheses are calculated using the thermal expansion data.

Parameter	V/V_0	T (K)	Error	Ref.
Thermal expansion	0.991–1.054	50–1300	<3%	19
Bulk modulus	(1.000–1.047)	300–1200	1%	15
	(0.990–1.000)	0–300	<1.5%	20
Specific heat	(1.000–1.054)	300–1300	~5%	21
	(0.991–1.000)	50–300	~2%	22

where the subscript 0 and h denote the initial condition of the sample and the shock-compressed state on the Hugoniot respectively, and $\rho = 1/V$. P_h can be derived from Eq. (13)–(15) as a function of V/V_0, and the internal energy change, $E_h - E_0$, can be calculated by Eq. (16). Although Jamieson *et al.*[3] and Wang *et al.*[16] provide comparable pressure values, Wang *et al.* used the shock compression data reported by Al'tshuler *et al.* in 1958,[17] which was later corrected in 1981.[13] Therefore, Wang *et al.* also tends to underestimate the pressure values, which are however later unfortunately employed in a different pressure scale modeling.[18]

The temperature in the shock-compressed state, T_h, can be calculated numerically along the Hugoniot using the following differential equation,

$$dT_h = -\gamma T_h \frac{dV}{V} + \frac{[(V_0 - V)dP + (P - P_0)dV]}{2C_v}. \quad (17)$$

For the numerical integration of Eq. (17), a fourth-order Runge-Kutta method was used in the initial a few steps, then

TABLE II. EOS parameters optimized for Au. C_0, S and Q are the parameters to represent the Hugoniot $U_s - u_p$ relationship in quadratic form as $U_s = C_0 + S u_p + Q u_p^2$.

Parameters	This work	Previous studies	References
$\rho_{0,300K}$, Mg/m^3	19.32		8
$B_{0,0K}$, GPa	180		14 and 20
$B_{0,300K}$, GPa	167.5	167	This work
$B'_{0,0K}$	5.61 ± 0.10		This work
$B'_{0,300K}$	5.79 (5.94)[a]	5.0–6.2[b]	This work
$\gamma_{0,300K}$	2.96	2.95–3.215[b]	This work
a	0.45 ± 0.09		This work
b	4.2 ± 0.6		This work
θ_0, K	170	165[c]	3
C_0, km/s	2.995	2.975–3.12[d]	15 and 23
S	1.653 ± 0.056	1.47–1.896[d]	This work
Q, (km/s)$^{-1}$	−0.013 ± 0.019	−0.309–0[d]	This work

[a]Fitted using the third-order Birch-Murnaghan equation, and the value in parenthesis is obtained from the Vinet equation[24]
[b]References 3 and 25–29.
[c]Reference 30.
[d]References 3, 8, 11, and 16.
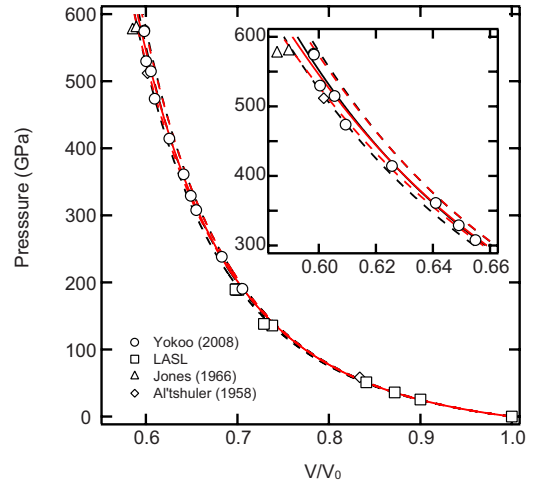
FIG. 2. (Color online) Experimental and calculated Hugoniot of Au. Black and red curves are obtained from the relationship of $U_s = 2.995 + 1.653 u_p - 0.013 u_p^2$ and calculated from the EOS parameters determined in this study, respectively. Dashed curves mean the uncertainties.

the Milne predictor-corrector method was used in the further steps.

C. Thermodynamic functions

Primary pressure standards should be determined only
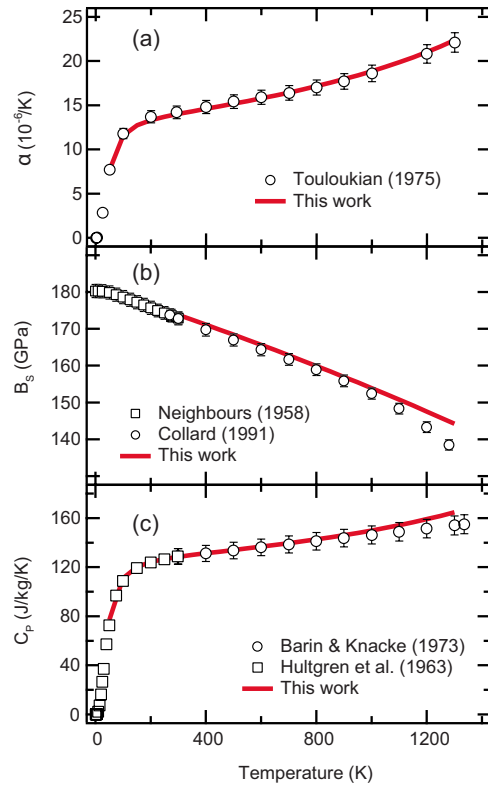
FIG. 3. (Color online) Comparisons of thermodynamic properties of Au calculated from our EOS parameters with the experimental data. (a) Linear thermal expansion coefficient (α), (b) adiabatic bulk modulus (B_s), and (c) specific-heat (C_p).

TABLE III. Isochores of Au, where V_0 is the ambient volume. Values in parentheses are for the first liquid state at each V/V_0.

V/V_0	T (K)							
	0	300	500	1000	1500	2000	2500	3000
1.00	−1.73	0.00	1.42	4.99	8.58	(12.18)		
0.98	1.92	3.59	4.98	8.49	12.02	(15.56)		
0.96	6.08	7.70	9.07	12.53	16.00	19.48	(22.99)	
0.94	10.83	12.41	13.76	17.16	20.59	24.02	(27.47)	
0.92	16.26	17.80	19.13	22.49	25.87	29.26	32.67	(36.10)
0.90	22.46	23.96	25.27	28.59	31.93	35.29	38.66	(42.06)
0.88	29.55	31.01	32.30	35.59	38.91	42.23	45.58	48.94
0.86	37.65	39.07	40.36	43.62	46.91	50.21	53.53	56.87
0.84	46.93	48.31	49.59	52.83	56.10	59.39	62.69	66.01
0.82	57.55	58.90	60.17	63.40	66.66	69.93	73.22	76.53
0.80	69.73	71.05	72.31	75.54	78.79	82.06	85.34	88.65
0.78	83.71	85.01	86.27	89.49	92.74	96.01	99.30	102.61
0.76	99.80	101.07	102.33	105.56	108.82	112.10	115.39	118.71
0.74	118.34	119.58	120.84	124.08	127.36	130.65	133.96	137.30
0.72	139.75	140.96	142.23	145.49	148.78	152.10	155.43	158.79
0.70	164.52	165.71	166.98	170.26	173.59	176.93	180.30	183.68
0.68	193.25	194.42	195.70	199.01	202.37	205.75	209.16	212.58
0.66	226.67	227.82	229.10	232.46	235.86	239.29	242.74	246.20
0.64	265.66	266.78	268.08	271.48	274.93	278.41	281.91	285.44
0.62	311.29	312.39	313.70	317.15	320.66	324.20	327.77	331.35
0.60	364.87	365.95	367.27	370.78	374.37	377.98	381.61	385.26

using experimental data measured independently from any other pressure standards. In addition to shock compression data, we used following scale-free 1 atm thermodynamic functions: thermal expansion α, adiabatic bulk modulus B_S, and specific heat C_p. 1 atm experimental data used in the EOS parameters optimization are summarized in Table I. Touloukian *et al.* compiled 30 different measurements of α with an accuracy of $\pm 3\%$ at temperatures up to 1300 K.[19] Neighbors and Alers determined B_S by single-crystal elastic wave velocity measurements at low temperatures with an accuracy of 1.5%,[20] and Collard and McLellan performed similar measurements at higher temperatures.[15] Uncertainties of 1% in B_S were assumed for the data of Collard and McLellan. For C_v, Hultgren *et al.*[21] and Barin and Knacke[22] compiled several previous measurements, and stated that the dispersions of the high- and low-temperature data were at most 5% and about 2%, respectively.

In the analysis of EOS, we used these thermodynamic data up to 1000 K, corresponding to $\sim 0.8T/T_m$ where T_m is the melting point, because the anharmonic effects become not negligible near the melting point. $B_{0,0K}$ was determined by using the Neighbors and Alers' value at 0 K of 180.3 GPa with corrections from the thermal expansion data of Touloukian *et al.* The Grüneisen parameter at 1 atm and 300 K, γ_0, was calculated using the thermodynamic experimental data with its definition,

$$\gamma = \frac{B_S \alpha V}{C_p} = \frac{B_T \alpha V}{C_v}, \tag{18}$$

where B_T is the isothermal bulk modulus. Finally, we used ρ_0 and Θ_0 reported in previous studies.[3,8]

D. Optimization of the EOS parameters

There are three adjustable parameters, the pressure derivative of B_0 at 0 K, $B'_{0,0K}$, and the constants a and b in the volume dependence of the Grüneisen parameter. γ_0 is obtained secondarily through the optimization procedures. We optimized all the parameters simultaneously using available experimental data of the thermal expansion, bulk modulus, specific heat at 1 atm and the Hugoniot. The parameters set were fully optimized by a steepest descent least-squares analysis with respect to the total pressures. The analytical procedure applied was described in a similar study on MgO (Ref. 9) in detail.

All the EOS parameters and their uncertainties determined from the simultaneous analysis are summarized in Table II with the values reported in other studies. The optimum $B'_{0,0K}$ was found to be 5.61 ± 0.10. The uncertainty of P_c was found to be ± 0.7 GPa ($\pm 1.0\%$) at $V/V_0=0.8$ ($P_c=70$ GPa), ± 2 GPa ($\pm 2\%$) at $V/V_0=0.7$ ($P_c=190$ GPa), and ± 7 GPa ($\pm 2\%$) at $V/V_0=0.6$ ($P_c=365$ GPa). The constants a and b for γ_{ph} are 0.45 ± 0.09 and 4.2 ± 0.6, respec-
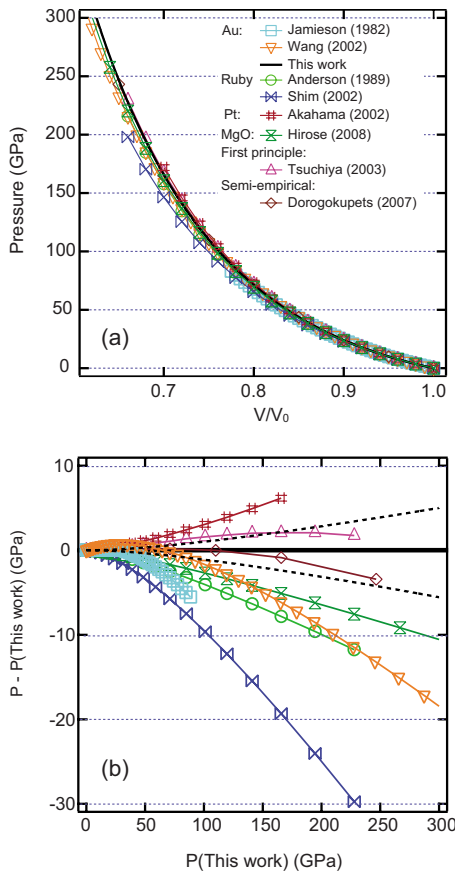
FIG. 4. (Color online) Calculated 300 K isotherms of Au. (a) Absolute pressure values of several models as a function of volume and (b) relative differences in the pressures as a function of the pressure given by our model.

tively, which yields uncertainties in γ_{ph} at most 7% in the entire volume range.

Figure 2 shows the Hugoniots calculated from the determined EOS model along with the raw shock compression data points.[8,11–13] The determined EOS model is in excellent agreement with the measured Hugoniot (Eq. (13)) within the margin of error over the entire pressure and volume ranges up to 600 GPa. A phase transition from fcc to hcp (Ref. 31) and melting[32] have been reported within this pressure range. However, we were unable to observe any kinks in the Hugoniot.[8] It is, in general, difficult to observe the melting reaction in shock compression experiments, since the volume changes associated with phase transitions are usually marginal at the extremely high-pressure condition.

The zero-pressure thermodynamic properties calculated from the determined EOS model are shown in Fig. 3. We can see good agreements of the calculated properties with the experimental data. Calculated thermal expansion coefficient is consistent with the experimental data at temperatures up to near the melting point (1337 K at 1 atm) with the deviation of the experimental data from the calculated curve of 1.4%. This suggests that the anharmonic effect is sufficiently small to ensure the validity of our EOS model. This anharmonic effect is generally expected to become less important with increasing pressure. For the bulk modulus and specific heat, the calculated values are also quite consistent with the experimental data at temperatures up to 1000 K with the deviations of 0.7% and 2.1%, respectively. Larger deviations of 2.9% (at 1200 K) and 6.5% (at 1300 K) are however found near the melting point maybe due to the anharmonic effects.

Pressure in our model contains each contribution from zero-temperature compression, phonon thermal vibration, and electronic thermal excitation. The electronic contribution in Au was reported to have no substantial effect on its Hugo-
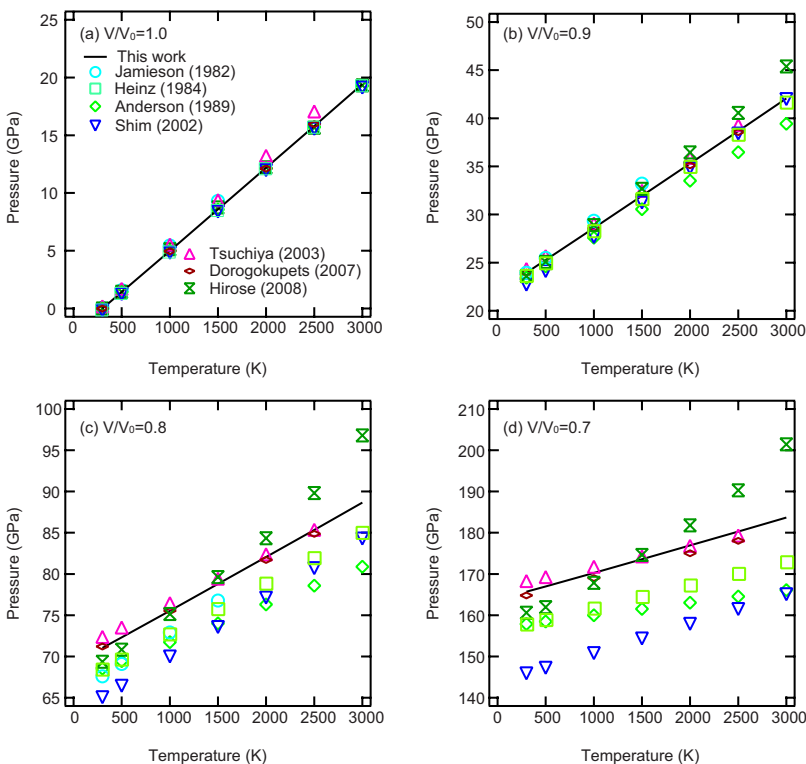
FIG. 5. (Color online) Isochores at $V/V_0=1.0$ (a), 0.9 (b), 0.8 (c), and 0.7 (d) up to 3000 K.
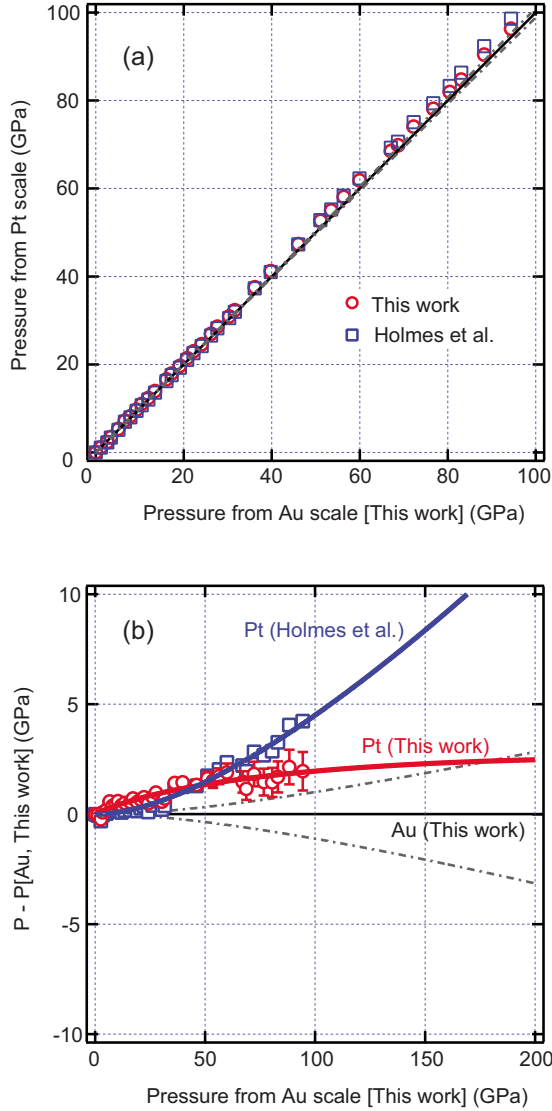
FIG. 6. (Color online) Comparison of the proposed Au and Pt scales and old Pt scale. (Ref. 4) (a) Absolute pressure values were examined using the volume data of Au and Pt simultaneously measured by Dewaele *et al.* (Ref. 18) Solid line means the condition $P_{Pt}=P_{Au}$. (b) Relative differences in these three scales. Dotted-dashed lines represent the uncertainty range of the present Au scale.

niot at low pressures, whereas at $V/V_0=0.6$, the Hugoniot reaches approximately 540 GPa and 21000 K, in which the electronic thermal pressure reaches 29 GPa (5.4% of the total pressure). This corresponds to 16% of the total internal energy, which means the conducting electron strongly affects the specific heat in this high-temperature condition.

We propose the *P-V-T* relationship in Table III as a primary pressure scale in the condition of $0 \leq T \leq 3000$ K and $0.6 \leq V/V_0 \leq 1.0$. Pressure uncertainty resulting from the Hugoniot uncertainty is estimated to be at most 2.0% up to 400 GPa.

III. COMPARISON WITH OTHER PRESSURE SCALES

300 K isotherms calculated from our EOS model and other models of Au are plotted in Fig. 4(a). The previous

TABLE IV. EOS parameters optimized for Pt. The U_s-u_p relationship is represented as $U_s=C_0+Su_p$.

Parameters	This work	Holmes	References
$\rho_{0,300K}$, Mg/m^3	21.40	21.45[a]	4
$B_{0,0K}$, GPa	288.4		38
$B_{0,300K}$, GPa	276.4	266	This work
$B'_{0,0K}$	5.05 ± 0.10		This work
$B'_{0,300K}$	5.12 (5.48)[b]	5.81[c]	This work
$\gamma_{0,300K}$	2.63	2.5[d]	This work
a	0.39 ± 0.08		This work
b	5.2 ± 1.1		This work
θ_0, K	230	230	4
C_0, km/s	3.635	3.641	39
S	1.543	1.541	This work

[a]Calculated from $V_0=101.9$ a.u.^{3}.
[b]Fitted using the third-order Birch-Murnaghan equation, and the value in parenthesis is obtained from the Vinet equation.[24]
[c]Using the Vinet equation.
[d]Using the Slater equation.[40]

models were on the basis of old shock compression data;[3,16] static measurements with other standards such as ruby scales,[26,27,33] Pt scale,[4] MgO scale;[34] first-principles calculations;[25,35] and semiempirical approaches compiling experimental thermodynamic data.[28,32] These models do not coincide with each other primarily due to the differences in their modeling process with or without using data measured depending on other scales. Differences in the pressure values determined from our EOS model and the previous models are plotted in Fig. 4(b) as a function of the pressure obtained from our EOS model. The dashed curves show the uncertainties of the Hugoniot. Indeed, we found that the primary source of the uncertainties in our analysis is from the uncertainty of the Hugoniot, in particular in high-pressure and high-temperature condition. The EOS models obtained from the first-principles calculations of Tsuchiya[25] and Souvatzis *et al.*[35] and from the semiempirical approach of Dorogokupets and Oganov[28] are in good agreement with our EOS model within the uncertainty.

In contrast, the EOS models proposed based on the old Hugoniot of Au[3,16] are found to substantially underestimate pressures at most 8% ($P \lesssim 80$ GPa) and 6% ($P \lesssim 300$ GPa), respectively, which are distinctly larger than the uncertainty of pressures in our model. These underestimations are, instead, mainly due to the differences in shock compression data used for modeling EOS as mentioned in Sec. II B.

Next, we compare our EOS model with the ruby scale determined based on the EOS of Cu, Ag, Pd, and Mo[2] and also with that based on the EOS of Cu and Ag.[36] This can be performed by comparing our model with the EOS models of Au determined based on the former ruby scale[26,33] and the other one determined based on the latter ruby scale.[27] Here, note that the 300 K isotherm of Heinz and Jeanloz is exactly the same as that of Anderson *et al.* We found that the ruby scale (Ref. 2) underestimates the pressure at most 5%, and the other ruby scale (Ref. 36) substantially underestimates

TABLE V. Isochores of Pt.

V/V_0	T (K)							
	0	300	500	1000	1500	2000	2500	3000
1.00	−1.76	0.00	1.52	5.37	9.25	13.15	17.09	(21.06)
0.98	4.18	5.89	7.38	11.16	14.97	18.81	22.67	(26.57)
0.96	10.90	12.55	14.02	17.74	21.49	25.27	29.07	32.92
0.94	18.48	20.09	21.53	25.20	28.91	32.63	36.39	40.18
0.92	27.06	28.62	30.04	33.67	37.33	41.02	44.73	48.48
0.90	36.76	38.28	39.68	43.28	46.90	50.56	54.24	57.96
0.88	47.73	49.21	50.61	54.18	57.78	61.40	65.06	68.76
0.86	60.16	61.61	63.00	66.54	70.13	73.74	77.38	81.06
0.84	74.26	75.68	77.06	80.59	84.17	87.77	91.41	95.08
0.82	90.28	91.66	93.04	96.57	100.14	103.74	107.38	111.05
0.80	108.48	109.85	111.22	114.75	118.33	121.94	125.58	129.26
0.78	129.22	130.56	131.93	135.48	139.07	142.70	146.35	150.05
0.76	152.88	154.20	155.57	159.14	162.75	166.40	170.08	173.80
0.74	179.94	181.23	182.61	186.20	189.84	193.52	197.24	200.98
0.72	210.93	212.20	213.59	217.21	220.90	224.61	228.37	232.15
0.70	246.53	247.77	249.17	252.83	256.56	260.33	264.13	267.97
0.68	287.51	288.74	290.14	293.85	297.64	301.46	305.32	309.21
0.66	334.83	336.03	337.45	341.21	345.06	348.95	352.87	356.83
0.64	389.62	390.80	392.23	396.06	399.98	403.94	407.94	411.97
0.62	453.28	454.44	455.89	459.79	463.78	467.83	471.90	476.02
0.60	527.51	528.64	530.11	534.08	538.17	542.30	546.47	550.69

pressure at most 12% ($P \lesssim 200$ GPa). This result supports previous comparisons between ruby scales.[18] A recent static x-ray diffraction experiment[37] determined the room-temperature isotherm of Au up to 123 GPa using pressure scales based on the ruby fluorescence. Even though their isotherm depends on the secondary scales, one of their B_0' values, which was determined using a ruby scale[28] incidentally coincides with our model.

Next, we compare our EOS model with the Pt scale.[4] This can be performed by comparing our model with the the simultaneous volume measurements of Au and Pt over 100 GPa.[7] Results indicate that the model of Pt gives the highest pressure for at 300 K among all the existing pressure scales, which is 3% higher than the pressure by our model at 150 GPa. This result strongly suggests significant overestimations of the pressure value in the Pt scale of Holmes *et al.*, although they state that their scale ensures only 10% accuracy for the static measurements.

We further compare our EOS model with the MgO scale determined based on the static volume measurements using the ruby scale.[34] This can be performed by comparing our model with the simultaneous volume measurements of Au and MgO.[29] Results indicate that the model of MgO gives 3% lower pressures up to 200 GPa compared with our EOS model.

Isochores of our model and the other models of Au are plotted at $V/V_0 = 1.0$, 0.9, 0.8, and 0.7 as a function of temperature from 300 to 3000 K in Fig. 5. This figure shows the differences in thermal pressure. At $V/V_0 = 1.0$, the difference

in pressure is basically due to the difference in the initial values of the Grüneisen parameter under ambient conditions, γ_0, ranging in 2.95–3.215. This causes a small fluctuation in pressure of ∼1 GPa up to 3000 K. In the compressed condition, the isochores widely scatter. The model of Anderson *et al.* gives the lowest pressure, while the model of Hirose *et al.* gives the largest pressure at the temperatures above 1500 K at $V/V_0 = 0.9$ and 0.8. The differences seen in the low-temperature range are caused mainly by the disagreements of zero-temperature compression curves, whereas those in the high-temperature range are mainly by the differences in thermal pressure. The Anderson *et al.*'s model was determined on the basis of the 300 K isotherm of the Heinz *et al.*'s model with applying the correction of anharmonic effects. Although the anharmonic effects should generally become smaller with increasing pressure, deviations in pressure calculated from this model are found to increase with increasing pressure. The Anderson *et al.*'s model quite likely underestimates the thermal pressure. The thermal pressure of the Hirose *et al.*'s model[29] becomes anomalously large compared to the other models, which was determined based on the EOS of MgO.[34] As a result, the EOS models of Tsuchiya[25] and Dorogokupets *et al.*[28] are in better agreement with our model in the entire temperature and volume range considered in this study, as the results of the 300 K isotherm.

IV. EOS MODEL OF PLATINUM

Pt has similar useful properties as Au for the pressure standard, apart from its low compressibility. A shock com-

pression experiment of Pt was conducted using a two-stage light-gas gun up to 660 GPa.[4] We determined a new EOS model of Pt by the same procedure as in Sec. II and compared it with the EOS model of Au.

All the EOS parameters of Pt and their uncertainties are summarized in Table IV. The thermodynamic properties at 1 atm from the determined EOS model of Pt are in good agreement with the experimental data in the entire temperature range.[19,22,38,39] The pressure derivative of the isothermal bulk modulus at 1 atm and 300 K, obtained from least-squared fitting to the third-order Birch-Murnaghan equation, is 5.12. This $B'_{0,300K}$ is smaller than the old value, 5.81,[4] and thus our EOS model gives lower pressures by at most 3%.

Pressures calculated from our EOS model and the Holmes *et al.*'s model of Pt are plotted in Fig. 6(a) as a function of the pressure value from our EOS model of Au. These are calculated using the simultaneously measured volume data of Au and Pt up to 100 GPa.[18] The solid and dashed lines represent the condition satisfying $P_{Pt}=P_{Au}$ and the uncertainty in the Au model of this work caused primarily by the Hugoniot, respectively. Figure 6(b) shows relative differences in the pressure values derived from the EOS models of Pt and Au. The condition $y=0$ means $P_{Pt}=P_{Au}$. Discrepancy between our Pt model and the previous model[4] is marginal below ~50 GPa but gradually increases to ~2 GPa (2%) at 100 GPa. On the other hand, the discrepancy between our Pt and Au models is 1.4 GPa (3%) at 50 GPa and slightly increases to 2 GPa (2%) at 100 GPa, but is almost unchanged at further pressures, 2 GPa (1%) at 200 GPa. Such discrepancies are found comparable to the uncertainty of the models. This mutual consistency displays reliability of our EOS

modeling of Au and Pt. The *P-V-T* relationship determined for Pt is summarized in Table V.

V. CONCLUSIONS

We redetermined the EOS parameters for Au and Pt by combining only pressure-scale-free experimental data based on the Mie-Grüneisen formulation with the Debye model and the Birch-Murnaghan equation. The electronic effects calculated by first-principles calculations were also included appropriately. Our model can successfully reproduce all the used experimental data. The new EOS model of Au gives relatively higher pressure values compared to the several previous models, while that of Pt gives lower pressures. These redetermined EOS of Au and Pt are mutually well consistent and their relative difference was found to be only ~2 GPa up to 200 GPa. This suggests reliability of our analytical procedure. The EOS models of Au and Pt reconstructed in this study are expected to be endurable as the primary pressure standards in the extremely broad *P*, *T* conditions.

*takut@sci.ehime-u.ac.jp

[1] D. C. Decker, J. Appl. Phys. **36**, 157 (1965).

[2] H. K. Mao, P. M. Bell, J. W. Shaner, and D. J. Steinberg, J. Appl. Phys. **49**, 3276 (1978).

[3] J. C. Jamieson, J. N. Fritz, and M. H. Manghanani, in *High-Pressure Research in Geophysics*, edited by S. Akimoto and M. H. Manghnani (Center for Academic Publications, Tokyo, 1982), p. 27.

[4] N. C. Holmes, J. A. Moriarty, G. R. Gathers, and W. J. Nellis, J. Appl. Phys. **66**, 2962 (1989).

[5] T. Irifune, N. Nishiyama, K. Kuroda, T. Inoue, M. Isshiki, W. Utsumi, K. Funakoshi, S. Urakawa, T. Uchida, T. Katsura, and O. Ohtaka, Science **279**, 1698 (1998).

[6] S. H. Shim, T. S. Duffy, and G. Shen, Nature (London) **411**, 571 (2001).

[7] Y. Akahama, H. Kawamura, and A. K. Singh, J. Appl. Phys. **92**, 5892 (2002).

[8] M. Yokoo, N. Kawai, Y. Hironaka, K. G. Nakamura, and K. Kondo, Appl. Phys. Lett. **92**, 051901 (2008).

[9] Y. Tange, Y. Nishihara, and T. Tsuchiya, J. Geophys. Res. **114**, B03208 (2009).

[10] T. Tsuchiya and K. Kawamura, Phys. Rev. B **66**, 094115 (2002).

[11] *Los Alamos Shock Hugoniot Data*, edited by S. P. Marsh (University of California Press, Berkeley, 1979).

[12] A. H. Jones, W. M. Isbell, and C. J. Maiden, J. Appl. Phys. **37**, 3493 (1966).

[13] L. V. Al'tshuler, A. A. Bakanova, I. P. Dudoladov, E. A. Dynin, R. F. Trunin, and B. S. Chekin, J. Appl. Mech. Tech. Phys. **22**, 145 (1981).

[14] S. N. Biswas, P. V. Klooster, and N. J. Trappeniers, Physica B **103**, 235 (1981).

[15] S. M. Collard and R. B. McLellan, Acta Metall. Mater. **39**, 3143 (1991).

[16] Y. Wang, R. Ahuja, and B. Johansson, J. Appl. Phys. **92**, 6616 (2002).

[17] L. V. Al'tshuler, K. K. Krupnikov, and M. K. Brazhnik, Sov. Phys. JETP **7**, 614 (1985).

[18] A. Dewaele, P. Loubeyre, and M. Mezouar, Phys. Rev. B **70**, 094112 (2004).

[19] Y. S. Touloukian, R. K. Kirby, R. E. Taylor, and P. D. Desai, in *Thermophysical Properties of Matter*, The TPRC Data Series Vol. 12 (Plenum, New York, 1975).

[20] J. R. Neighbours and G. A. Alers, Phys. Rev. **111**, 707 (1958).

[21] I. Barin and O. Knacke, *Thermochemical Properties of Inorganic Substances* (Springer, Berlin, 1973).

[22] R. Hultgren, R. L. Orr, P. D. Anderson, and K. K. Kelley, *Selected Values of Thermodynamic Properties of Metals and Alloys* (Wiley, New York, 1963).

[23] *Single Crystal Elastic Constants and Calculated Aggregated Properties: A Handbook*, edited by G. Simmon and H. Wang (MIT Press, Cambridge, MA, 1971).

[24] P. Vinet, J. Ferrante, J. H. Rose, and J. R. Smith, J. Geophys. Res. **92**, 9319 (1987).

[25] T. Tsuchiya, J. Geophys. Res. **108**, 2462 (2003).

[26] D. L. Heinz and R. Jeanloz, J. Appl. Phys. **55**, 885 (1984).

[27] S. H. Shim, T. S. Duffy, and K. Takemura, Earth Planet. Sci. Lett. **203**, 729 (2002).

[28] P. I. Dorogokupets and A. R. Oganov, Phys. Rev. B **75**, 024115 (2007).

[29] K. Hirose, N. Sata, T. Komabayashi, and Y. Ohishi, Phys. Earth Planet. Inter. **167**, 149 (2008).

[30] J. E. Zimmerman and L. T. Crane, Phys. Rev. **126**, 513 (1962).

[31] L. Dubrovinsky, N. Dubrovinskaia, W. A. Crichton, A. S. Mikhaylushkin, S. I. Simak, I. A. Abrikosov, J. S. de Almeida, R. Ahuja, W. Luo, and B. Johansson, Phys. Rev. Lett. **98**, 045503 (2007).

[32] C. W. Greeff and M. J. Graf, Phys. Rev. B **69**, 054107 (2004).

[33] O. L. Anderson, D. G. Isaak, and Y. Yamamoto, J. Appl. Phys. **65**, 1534 (1989).

[34] S. Speziale, C. S. Zha, T. S. Duffy, R. J. Hemley, and H. K. Mao, J. Geophys. Res. **106**, 515 (2001).

[35] P. Souvatzis, A. Delin, and O. Eriksson, Phys. Rev. B **73**, 054110 (2006).

[36] H. K. Mao, J. Xu, and P. M. Bell, J. Geophys. Res. **91**, 4673 (1986).

[37] K. Takemura and A. Dewaele, Phys. Rev. B **78**, 104119 (2008).

[38] R. E. Macfarlane, J. A. Rayne, and C. K. Jones, Phys. Lett. **18**, 91 (1965).

[39] S. M. Collard and R. B. McLellan, Acta Metall. Mater. **40**, 699 (1992).

[40] S. C. Slater, Phys. Rev. **57**, 744 (1940).